19th Brazilian Congress of Thermal Sciences and Engineering
November 6th–10th, 2022, Bento Gonçalves - RS - Brazil

ENC-2022-0158
Analysis of the boundary layer transition process caused by a gap

Felipe Oliveira Aguirre[1]
Marlon Sproesser Mathias[2]
Marcello A. F. Medeiros[1]
felipe.aguirre@usp.br
marlon.mathias@usp.br
marcello@sc.usp.br
[1]São Carlos School of Engeneering - University of São Paulo
[2]Institute of Advanced Studies - USP

Abstract. *The interaction of the boundary layer with small surface irregularities has been studied in several contexts. Several studies reveal that some configurations of gaps, also called small cavities, can induce boundary-layer disturbances due to the presence of unstable hydrodynamic modes. The literature presents results where, in some scenarios, the presence of gaps can induce boundary layer transition through the bypass transition phenomenon. To better understand this scenario, a representative case was chosen, where the transition occurs near the gap. For this case, it was analyzed how the unsteady modes predicted in linear stability theory behave in the flow. Initially, it was investigated how these modes behave inside the cavity, interacting and subsequently being convected out of the cavity. Subsequently, the convected structures were followed along the domain, to understand if there is memory of the flow structures present inside the cavity. We observed the presence of unstable two-dimensional modes in the mixing layer, known as Rossiter modes, and unstable three-dimensional modes inside the cavity, known as centrifugal modes, which are subsequently convected into the boundary layer downstream of the cavity. Analyzing the transition region, where the flow changes from laminar to turbulent, it was possible to notice that the Rossiter and Centrifugal modes are present in this region, interacting with each other. Finally, through the analysis of the turbulent region, it is possible to note the presence of memory of the centrifugal modes present in the cavity, as well as the presence of residual modes with a frequency close to the Rossiter modes.*

Keywords: *boundary layer, flow instability, transition to turbulence, DNS, open cavity*

1. INTRODUCTION

In this work we study a boundary layer flow over na open cavity whose dimensions are, usually, one order of magnitude larger than the boundary layer thickness.

According to more recent work, the situation closest to the reality of an aircraft in flight would be the introduction of a disturbance in the boundary layer upstream of the cavity or roughness,this is a way of imitating nactually ocurring Tollmien-Schlichting waves. Therefore, the irregularities should not act as generators of the disturbance, but instead modify the waves already present in the flow Crouch and Ng (2000); Plogmann *et al.* (2014); de Paula *et al.* (2017). Taking into account this context of cavities more in line with reality, Crouch *et al.* (2020) identified a parametric region in their experiments where an abrupt change of behavior of the flow occurs, where a phenomenon of anticipation of the transition point occurs abruptly, this is called by *bypass transition*.

Recent studies by the group have observed that in cases where *bypass transition* occurred, both two-dimensional unsteady modes (Rossiter modes) and three-dimensional unsteady modes (Centrifugal modes) were found Mathias (2021).

The Rossiter modes, in short, are self-sustained disturbances in the mixing layer and are amplified up to the trailing edge, where when they collide with the trailing edge, they generate an acoustic wave, which returns through the interior of the cavity exciting the mixing layer once more Rossiter (1964). The centrifugal modes, on the other hand, are the modes connected to the recirculation inside the cavity, with defined spanwise periods, therefore being three-dimensional Bres and Colonius (2008). It was also possible to observe similar behavior for the linear instability analysis, for Mach 0.5, well above the Mach at which the experiment was performed (below 0.1).

2. METHODOLOGY

For the present study, an unstable case was chosen. This case was chosen based on previous studies, where a parameter sweep was performed resulting in the choice of an intermediate case to two cases studied earlier in the group (Mathias and Medeiros, 2019). The case in question was non-dimensionalized by the displacement thickness of the boundary layer at the cavity's landing edge (δ_0^*), and by the free-flow velocity. Also follows the following definitions: length-depth ratio (L/D) equal to 2, as well as a depth of 6.11 δ^*. The cavity is situated at a Red* of 734, with Mach equal to 0.5.

The case was simulated using a Direct Numerical Solver, or DNS. The DNS was developed by the group and written in Fortran 90, and it solves Navier Stokes' compressible equations. For the spatial resolution, the sixth order Compact Finite Difference Schemes with Spectral-like method was used, and for the buffer zones, the explicit fourth-order method was used. For the temporal resolution, the fourth-order Runge-Kutta method was used. A Fig. 1 contains a section of the X Y plane, to exemplify the operation of the mesh

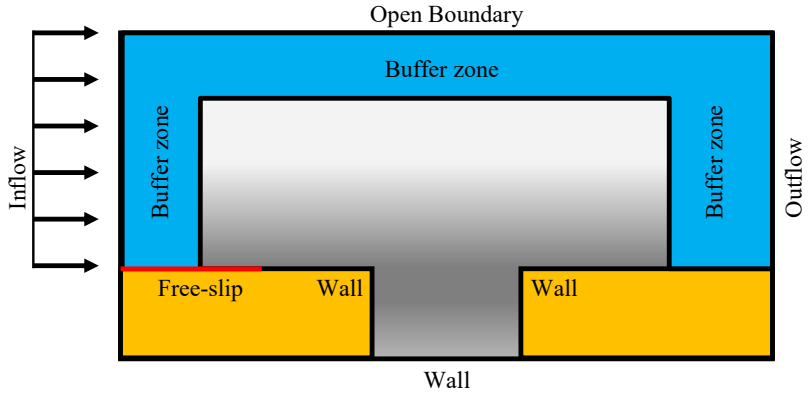

Figure 1. Illustrative image of the computational domain, the bufferzones are in blue.

With the stability analysis, it was possible to observe the unstable modes, as well as to set up the domain so that it was possible to have a resolution of 4 points per period of the mode with the shortest unstable wavelength, as well as a domain with 4 periods of the mode with the longest unstable wavelength.

With the results obtained in DNS, analyses were performed to verify if the downstream flow in the cavity was turbulent, laminar, or something in between. For this study the comparative coefficient of friction (C_f) and the wall law were used. Two-dimensional sections of the flow were also used to analyze this flow, as well as three-dimensional Q-Criterium plots to visualize the physical characteristics of the flow.

To better understand the transition, it is necessary to analyze not only whether the case has transitioned or not, it is necessary to look carefully at the modes present in each part of the domain, for this, spectrum analyses were performed to understand whether the modes predicted in the LST are present in the cavity, as well as whether the modes present in the cavity also appear downstream, as well as to what extent they are present and how they change as we move towards the end of the domain.

3. RESULTS

The case was chosen because it was a case between a marginally unstable and a fully unstable case (Mathias and Medeiros, 2019), so it was necessary to initially determine which modes were unstable, and with that determine a domain in the Z direction sufficient to capture all the modes present in the flow. A Linear Stability Theory analysis, or LST, was performed and determined the major unstable modes for each span-wise wave number β chosen. The modes found are shown in Fig. 2. Initially, looking at the amplification, we have that for β/π between 0.1 and 1 we have several unstable modes, these being centrifugal modes, as well as the presence of a two-dimensional mode (Rossiter mode) for $\beta/\pi = 0$. Looking now at the frequency, we find 3 types of centrifugal modes, two types with frequency different from 0 (mode II and mode III (Bres and Colonius, 2008)) and a stationary centrifugal mode dominating the region of $\beta/\pi > 0.5$.

To facilitate the comparison between the physical domain and the spectral domain, we will change the span-wise wave number from β to $1/\lambda$, given by $1/\lambda = \beta/2\pi$, where $1/\lambda$ is equivalent to the inverse of the wavelength in the span-wise direction. The spanwise wavenumber expected for the centrifugal 1 is around $0.25 \leq 1/\lambda \leq 0.5$. For the centrifugal 2 is expected a spanwise wavenumber around $0.15 \leq 1/\lambda \leq 0.2$. Finally the centrifugal 3 is expeted for $0.7 \leq 1/\lambda \leq 0.1$.

For the mixing layer, Fig. 3, where we can observe the concentration of energy in the range predicted by the LST for Rossiter mode 1. We can observe the presence of the Rossiter mode 1 harmonic mainly in the region between the center of the gap and the third-quarter of the gap.

Filtering the high-frequency modes in the mixing layer, Fig. 4, the deformation of the velocity fluctuation suggests an

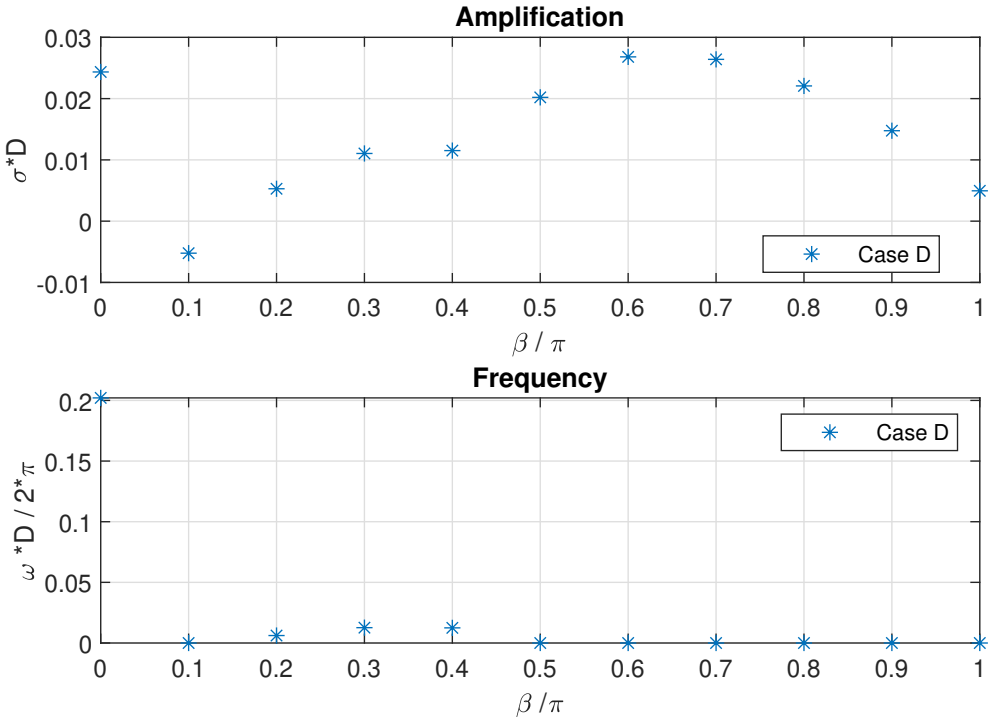

Figure 2. Figure showing the amplifications of the most unstable mode for each β of the scan, in the top figure is present the amplification and in the bottom figure is the frequency of these modes.

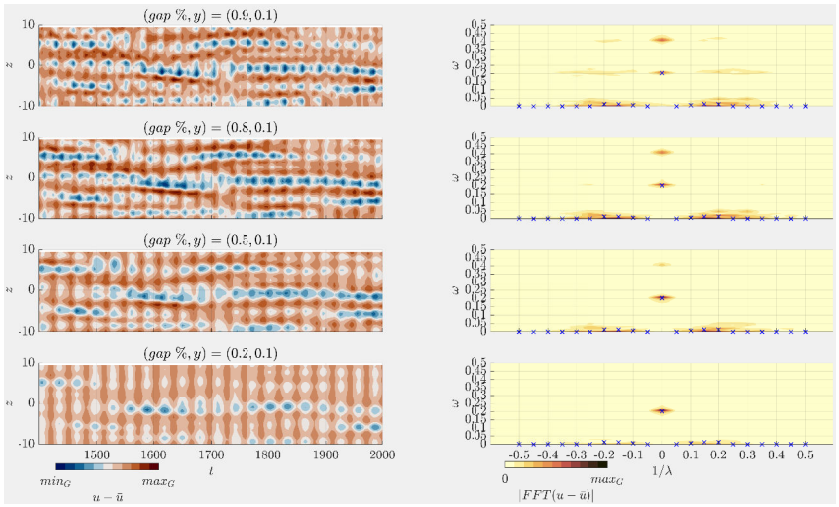

Figure 3. In the left column we have the physical domain and in the right column the respective 2D spectral domain for for different percentages of the gap in X, at a height of $Y \approx 0.1$. The blue markings are the most unstable modes predicted by the LST for each value of $1/\lambda$.

interaction between different modes in the region near the trailing edge and the center of the gap. For the leading edge, we can see that the modes move slowly in the spanwise direction over time. Also we can notice a high concentration of energy mainly in the range of the C1 modes. The distribution of energy in the frequency band of the C2 and C3 modes can also be noted, despite the energy being concentrated mainly in the C1 mode.

Analyzing the bottom of the gap, Fig. 5, for the region of $Y \approx -5.5$, we can observe the concentration of energy in the range predicted by the LST for Rossiter mode 1. Again, due to the energy concentrated in the Rossiter mode region, it interferes with the visualization of the low frequency modes.

Filtering the high-frequency modes, Fig. 6, we can see that in the region near the gap walls, we have velocities fluctuations, which move over time in the spanwise direction. We can notice that for regions further to the center of the gap, we have changes in the structures over time, suggesting the interaction between different types of modes. In Fig. 6 we can observe the concentration in centrifugal mode 1 mainly in the initial three-quarters of the gap. It can be noted the

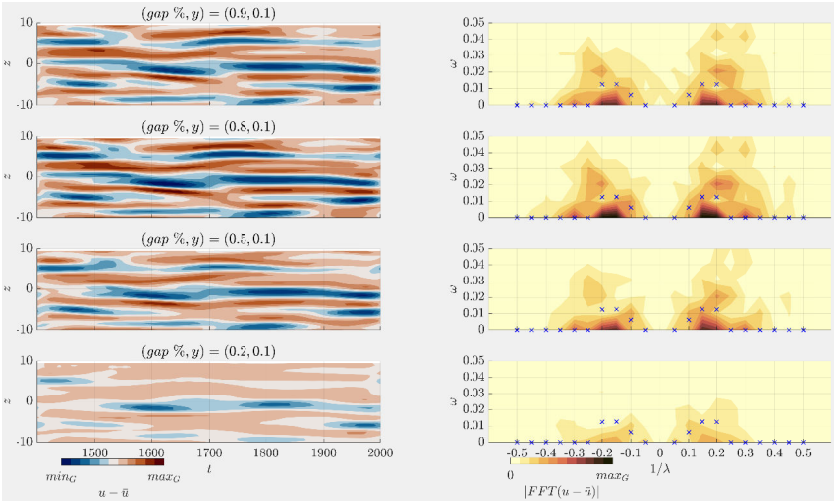

Figure 4. In the left column we have the physical domain and in the right column the respective 2D spectral domain for for different percentages of the gap in X, at a height of $Y \approx 0.1$, filtering the high-frequencies. The blue markings are the most unstable modes predicted by the LST for each value of $1/\lambda$.

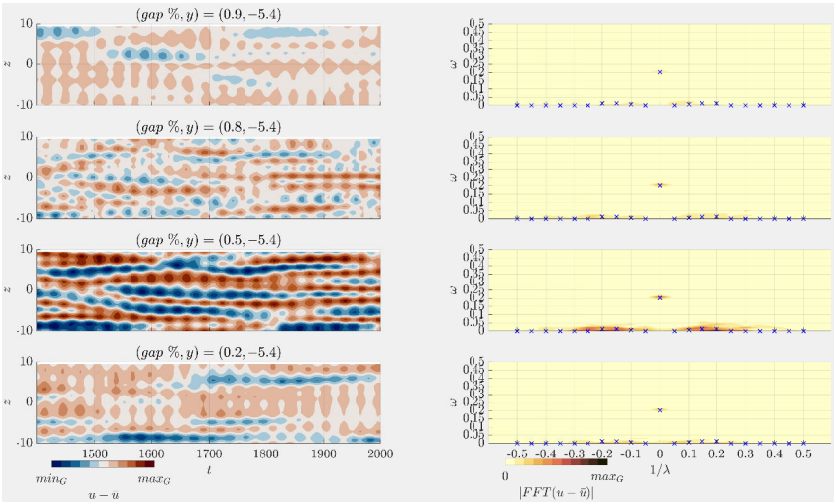

Figure 5. In the left column we have the physical domain and in the right column the respective 2D spectral domain for for different percentages of the gap in X, at a height of $Y \approx -5.4$. The blue markings are the most unstable modes predicted by the LST for each value of $1/\lambda$.

presence of low-frequency modes in the range of $1/\lambda$ is equivalent to modes C2 and C3.

To better understand the behavior of the gap, we can analyze Fig. 7, to try to better understand the behavior of the gap. In it we can again observe the presence of three-dimensional structures in Q-criterium, as well as two-dimensional structures being convected from the gap.

From the two-dimensional cuts, as can be seen in Fig. 8, the transition region is between the cavity and approximately $X = 365$.

Now analyzing the modes downstream of the gap, the velocity begins to oscillate more and more in the spanwise direction, until-we reach the turbulent region. In Fig. 9, close to the plate, for the region of the trailing edge, the energy is concentrated both in the centrifugal modes of the cavity and in the Rossiter mode predicted in the LST, which remain until the central region of the transition zone, where the modes tend to concentrate in a low-frequency band, with a spread to $1/\lambda$ in the region of the frequency of the mode of Rossiter. As we approach the turbulent region, the energy begins to spread, eventually covering a wide range of wavenumbers and frequencies.

Filtering the high-frequency modes, we can notice that in the region close to the trailing edge of the gap, in Fig. 10, the highest energy mode is the stationary centrifugal mode, as predicted in LST, downstream to the gap, there is a spreadin to larger . As we get to the end of the transition region, we have energy scattering for smaller $1/\lambda$, and in the turbulence region, there is a scatter to several frequencies.

Analyzing the modes present in the region of $Y \approx 1$, Fig. 11, we have that for the region of the trailing edge of the cavity, the energy is more concentrated in the Rossiter mode, downstream of the gap, in the transition region, we have an

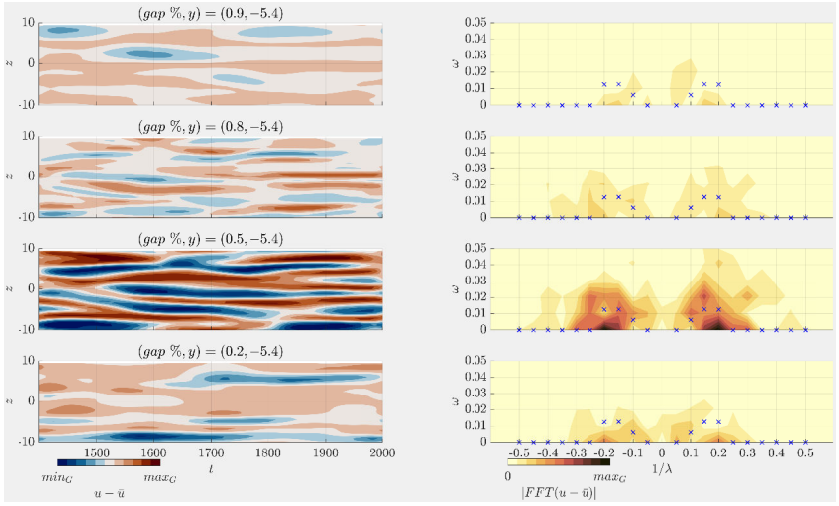

Figure 6. In the left column we have the physical domain and in the right column the respective 2D spectral domain for for different percentages of the gap in X, at a height of $Y \approx -5.4$, filtering the high-frequencies. The blue markings are the most unstable modes predicted by the LST for each value of $1/\lambda$.

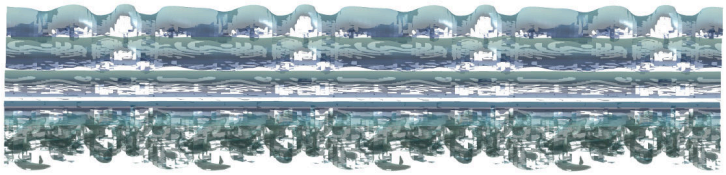

Figure 7. Q-criterium isosurfaces snapshots, where it is possible to observe the vortices present inside the gap and convected. Domain in spanwise direction was replicated 4 times for better visualization. The figure is in the gap region.

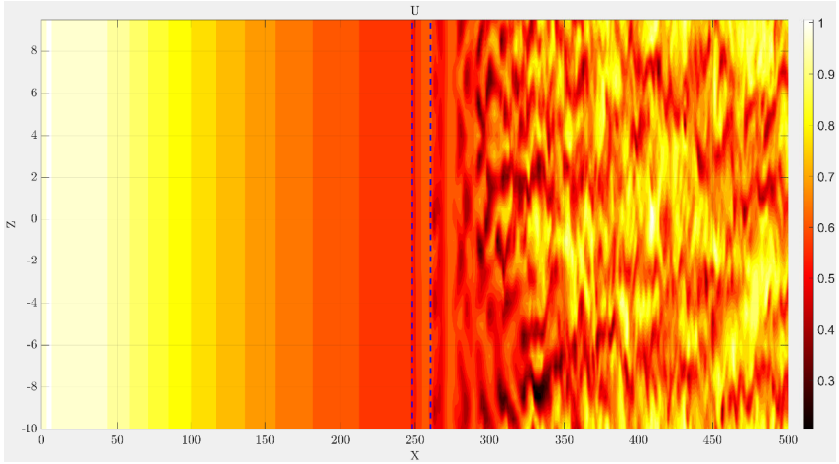

Figure 8. Flow cut in the $Y = 1$ plane to the velocity component U, at time $t = 1000$.

energy spread predicted in the LST, mainly of the centrifugal modes, and in the region of the frequency of the Rossiter mode and its first harmonic.

As we reach the end of the transition region, the energy spreads to other frequencies, and finally, for the fourth station, we have an even greater spread of the spectrum, both in frequency and in wave number.

As in Fig. 10, filtering the high-frequency modes in Fig. 12, as we move downstream from the gap, the velocity

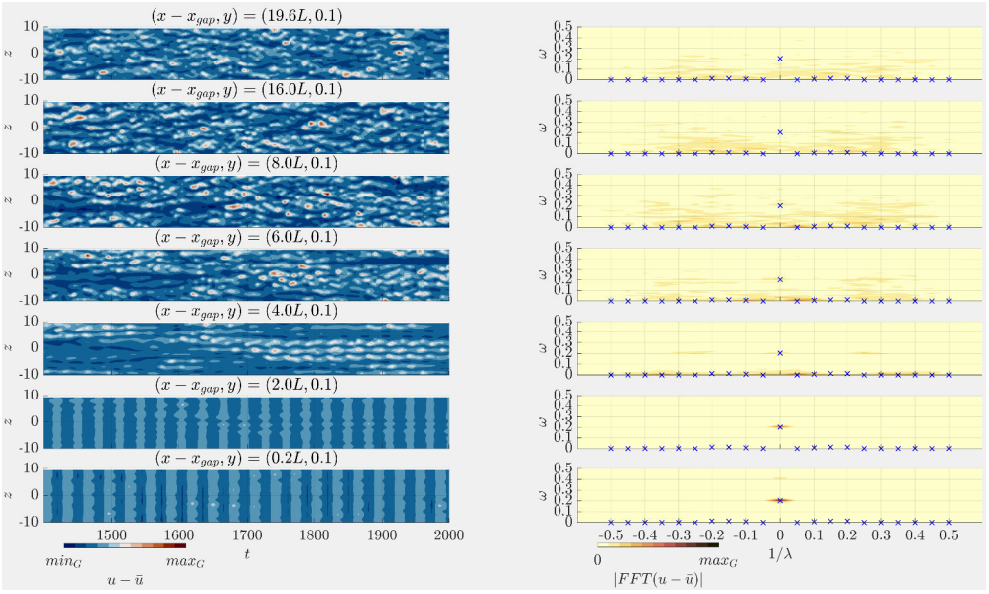

Figure 9. In the left column we have the physical domain and in the right column the respective 2D spectral domain for different positions of X downstream of the gap, at a height of $Y = 0.1$. For this case $L/\delta^* = 12.22$. The blue markings are the most unstable modes predicted by the LST for each value of $1/\lambda$.

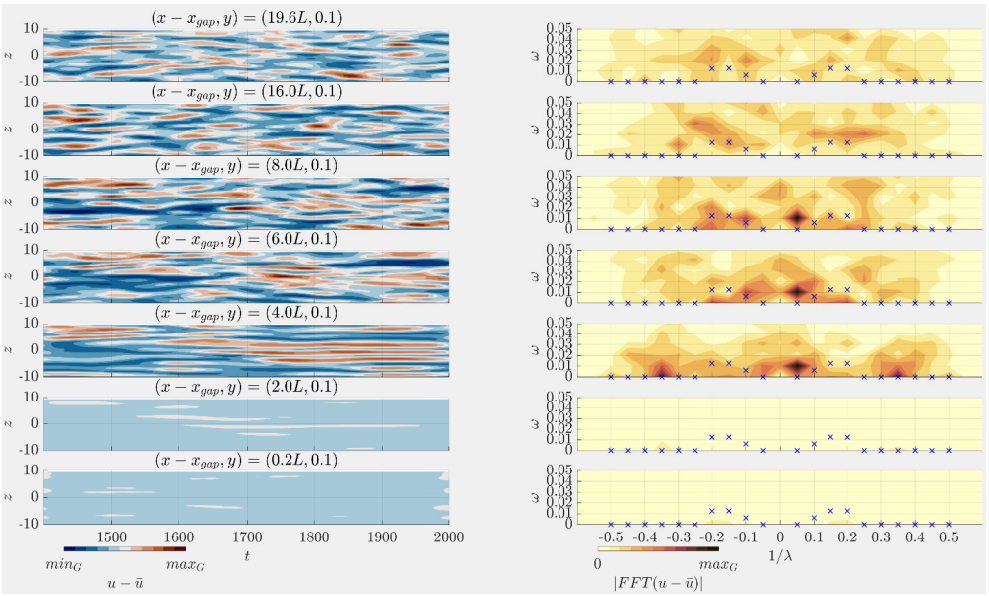

Figure 10. In the left column we have the physical domain and in the right column the respective 2D spectral domain for different positions of X downstream of the gap, at a height of $Y = 0.1$, without the highest frequencies. For this case $L/\delta^* = 12.22$. The blue markings are the most unstable modes predicted by the LST for each value of $1/\lambda$.

fluctuations begin to oscillate more and more in the spanwise direction, as well as more frequently over time when we reach the region turbulent. In Fig. 12, we have that the centrifugal modes present in the gap region, evolve to modes with higher wavenumbers, and later, the energy returns to concentrate on modes with lower spanwise wavenumber the end of the transition region. However, in the turbulent region, the energy spreads to various frequencies, maintaining the gap wavenumber region.

4. CONCLUSION

An analysis of an unstable case was carried out due to the possibility of studying the boundary layer transition. For this case, the analysis of the instabilities modes found in the cavity during DNS was carried out, compared with those predicted in the theory of linear stability (LST), and also the study of how these modes present in the flow behave during the transition process of the boundary layer.

The wall law, as well as the friction coefficient, were used to confirm the transition process, as well as the help of

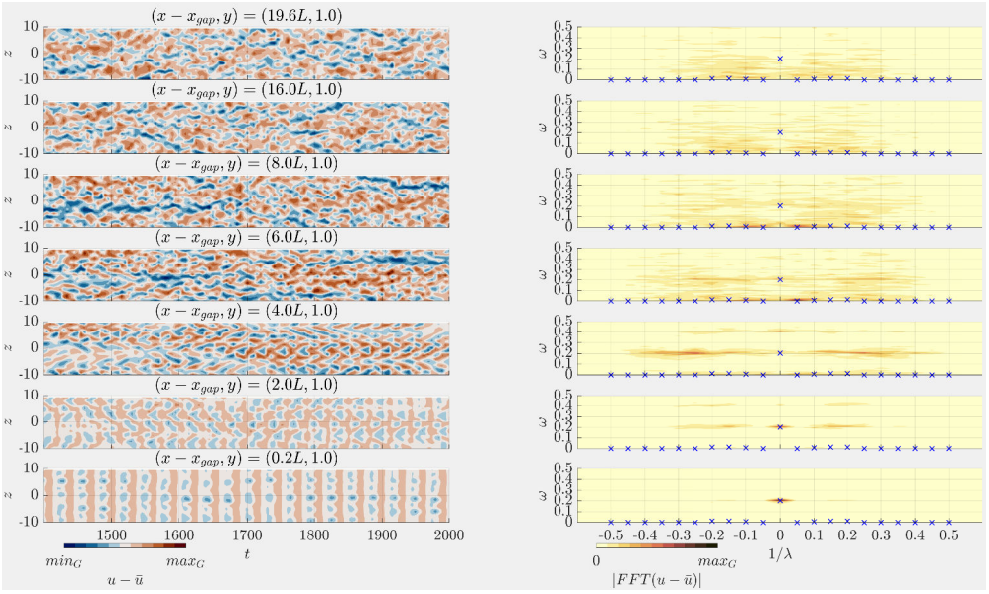

Figure 11. In the left column we have the physical domain and in the right column the respective 2D spectral domain for different positions of X downstream of the gap, at a height of $Y = 1$. For this case $L/\delta^* = 12.22$. The blue markings are the most unstable modes predicted by the LST for each value of $1/\lambda$.

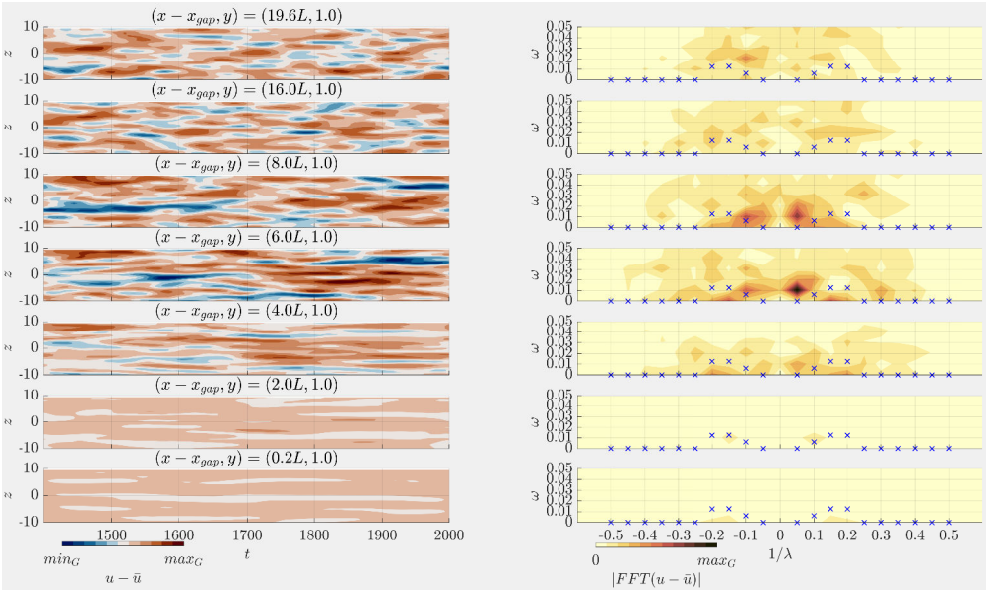

Figure 12. In the left column we have the physical domain and in the right column the respective 2D spectral domain for different positions of X downstream of the gap, at a height of $Y = 1$,without the highest frequencies. For this case $L/\delta^* = 12.22$. The blue markings are the most unstable modes predicted by the LST for each value of $1/\lambda$.

two-dimensional cuts and figures using the Q-criterium to visualize the structures and try to understand the behavior. It was found that turbulence was present from the point $X = 350$, and that it extended to the end of the domain. With the figures of the flow and vortices, it was possible to notice that there is a transition region, where the flow is not fully turbulent, but also not laminar.

The LST predicted the existence of centrifugal modes of type II and III for the region of $0 < \beta/\pi < 0.5$ as the most unstable for these betas, while for $0.5 < \beta/\pi < 1$ the presence of stationary centrifugal modes were predicted as the most unstable for these betas. For $\beta/\pi = 0$ a Rossiter mode was expected. However, in DNS, stationary modes were not observed, with the flow dominated only by non-stationary modes. The centrifugal modes of $0 < \beta/\pi < 0.5$ have a frequency similar to that predicted in the LST, and the observed Rossiter mode is also similar to that expected by the LST.

The 2D spectra also revealed that the 2D modes underwent a three-dimensionalization in the same β/π region as the existing centrifugal modes. It was also observed that during the transition region it is possible to observe the presence of the modes found in the gap. Another important point observed is that in the turbulent region, despite the frequency

scattering, the spectrum remains in the β/π region of the cavity modes.

Finally, using the observed spectra and using the Q-criterium figures to help the interpretation, we can see that the interaction of two-dimensional modes with the three-dimensional ones present in the cavity is responsible for generating the three-dimensionality observed in the turbulent region of the boundary layer. Nothing can be said about which mode is responsible for the transition, but it is reasonable to say that the interaction of unstable centrifugal modes with also unstable Rossiter modes can generate three-dimensionality in the boundary layer, which can therefore lead to the boundary layer transition.

5. ACKNOWLEDGEMENTS

M.S.M is sponsored by FAPESP (grant no. 2018/04584-0). M.A.F.M. is sponsored by CNPq/Brazil (grant no. 307956/2019-9), sponsored by FAPESP (grant no. 2019/15336-7) and the US Air Force Office of Scientific Research (AFOSR) for grant FA9550-18-1-0112, managed by Dr. Geoff Andersen from SOARD; the University of Liverpool for the access to the Barkla cluster, provided by Prof. Vassilios Theofilis; and the Center for Mathematical Sciences Applied to Industry (CeMEAI) funded by São Paulo Research Foundation (FAPESP/Brazil), grant 2013/07375-0, for access to the Euler cluster, led by Prof. José Alberto Cuminato.

6. REFERENCES

Bres, G.A. and Colonius, T., 2008. "Three-dimensional instabilities in compressible flow over open cavities". *JOURNAL OF FLUID MECHANICS*, Vol. 599, pp. 309–339. ISSN 0022-1120. doi:10.1017/S0022112007009925.

Crouch, J.D. and Ng, L.L., 2000. "Variable n-factor method for transition prediction in three-dimensional boundary layers". *AIAA Journal*, Vol. 38, No. 2, pp. 211–216. doi:10.2514/2.973. URL `https://doi.org/10.2514/2.973`.

Crouch, J.D., Kosorygin, V.S. and Sutanto, M.I., 2020. *Modeling Gap Effects on Transition Dominated by Tollmien-Schlichting Instability*, AIAA AVIATION FORUM. doi:10.2514/6.2020-3075. URL `https://arc.aiaa.org/doi/abs/10.2514/6.2020-3075`.

de Paula, I.B., Würz, W., Mendonça, M.T. and Medeiros, M.A.F., 2017. "Interaction of instability waves and a three-dimensional roughness element in a boundary layer". *Journal of Fluid Mechanics*, Vol. 824, p. 624–660. doi: 10.1017/jfm.2017.362.

Mathias, M.S., 2021. *Computational study of the hydrodynamic stability of gaps and cavities in a subsonic compressible boundary layer*. Ph.D. thesis, University of São Paulo.

Mathias, M. and Medeiros, M.F., 2019. *Global instability analysis of a boundary layer flow over a small cavity*, AIAA Aviation 2019 Forum. doi:10.2514/6.2019-3535. URL `https://arc.aiaa.org/doi/abs/10.2514/6.2019-3535`.

Plogmann, B., Würz, W. and Krämer, E., 2014. "On the disturbance evolution downstream of a cylindrical roughness element". *Journal of Fluid Mechanics*, Vol. 758, p. 238–286. doi:10.1017/jfm.2014.499.

Rossiter, J.E., 1964. "Wind-tunnel experiments on the flow over rectangular cavities at subsonic and transonic speeds". *Reports and Memoranda No. 3438 - Aeronautical Research Council - Ministry of Aviation*.

7. RESPONSIBILITY NOTICE

The authors are solely responsible for the printed material included in this paper.